# S- and p-wave structure of S = -1 meson-baryon scattering in the resonance region

Supported by DOE SCGSR, NSF (PIF No.1415459, CAREER PHY-1452055),
DOE DE-AC05-06OR23177 & DE-SC0016582), DFG MA 7156/1-1.

Daniel Sadasivan

Maxim Mai

Michael Doring

# Motivation

# What is a Resonance

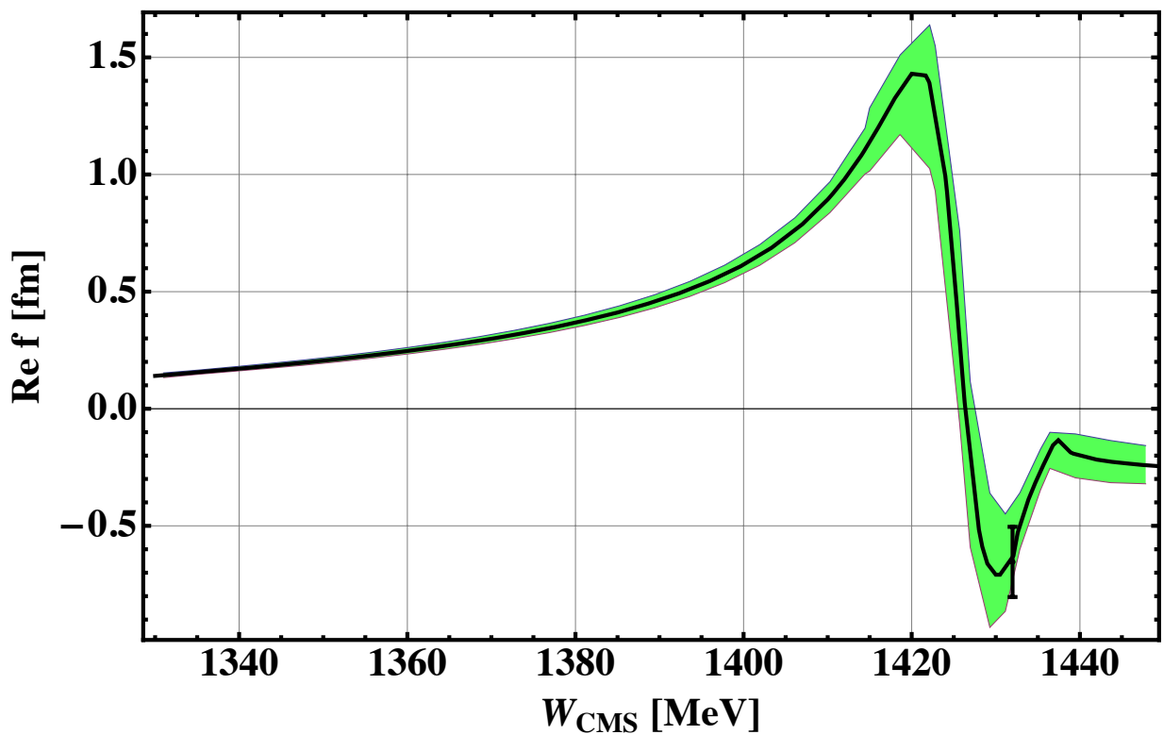


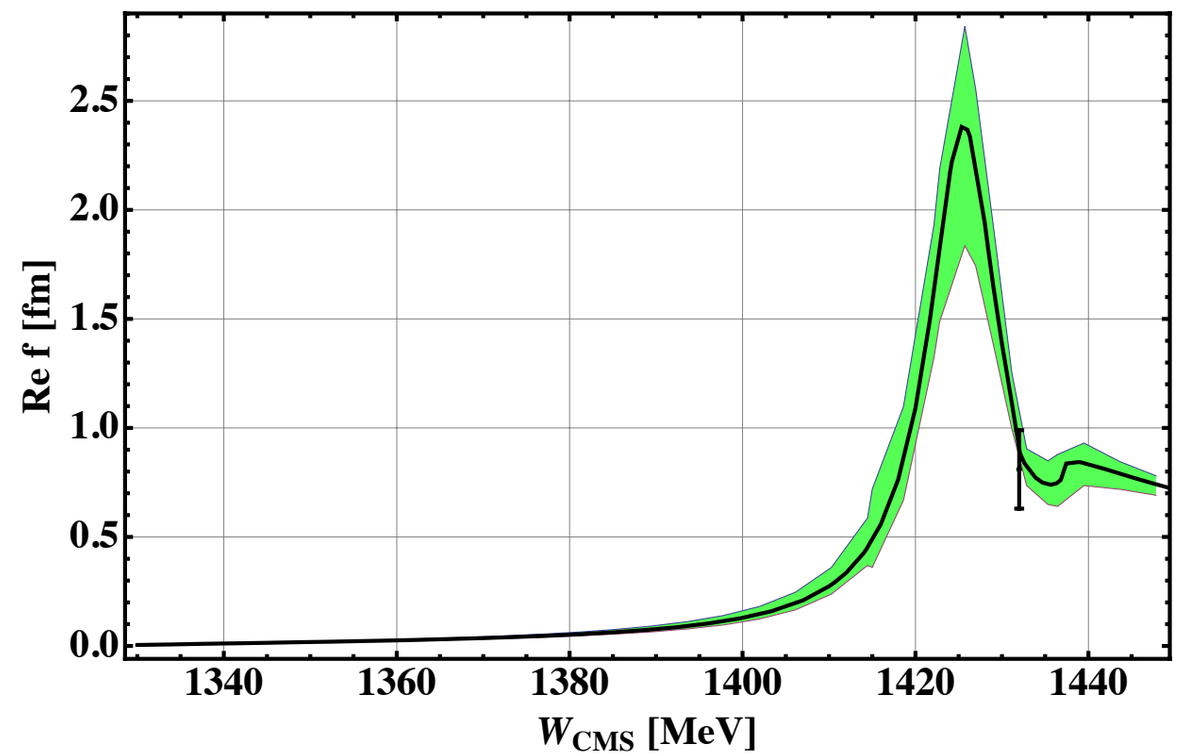


- Seen in peak at a certain energy in scattering cross sections.
- Assigned to certain quantum numbers.
- Can be studied through analytic continuation
- Useful to relate results to other theories like quark models and lattice QCD.

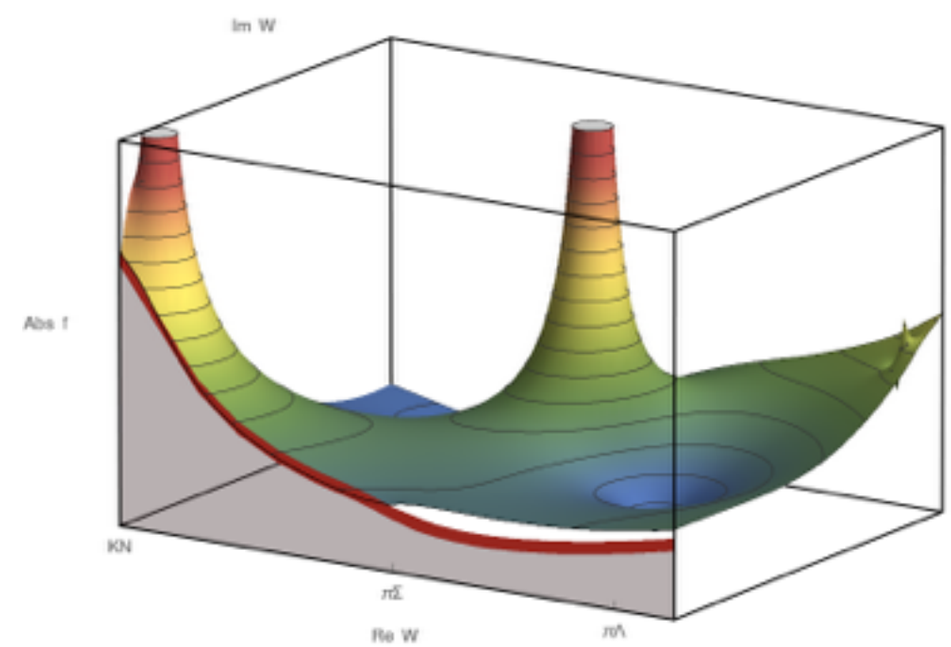

# Resonances We Are Looking For

Citation: C. Patrignani et al. (Particle Data Group), Chin. Phys. C, 40, 100001 (2016) and 2017 update

## $\Lambda(1405)\ 1/2^-$

$I(J^P) = 0(\frac{1}{2}^-)$ Status: ****

In the 1998 Note on the $\Lambda(1405)$ in PDG 98, R.H. Dalitz discussed the S-shaped cusp behavior of the intensity at the $N$-$\overline{K}$ threshold observed in THOMAS 73 and HEMINGWAY 85. He commented that this behavior "is characteristic of $S$-wave coupling; the other below threshold hyperon, the $\Sigma(1385)$, has no such threshold distortion because its $N$-$\overline{K}$ coupling is $P$-wave. For $\Lambda(1405)$ this asymmetry is the sole direct evidence that $J^P = 1/2^-$."

A recent measurement by the CLAS collaboration, MORIYA 14, definitively established the long-assumed $J^P = 1/2^-$ spin-parity assignment of the $\Lambda(1405)$. The experiment produced the $\Lambda(1405)$ spin-polarized in the photoproduction process $\gamma p \to K^+\Lambda(1405)$ and measured the decay of the $\Lambda(1405)$(polarized) $\to \Sigma^+$(polarized)$\pi^-$. The observed isotropic decay of $\Lambda(1405)$ is consistent with spin $J = 1/2$. The polarization transfer to the $\Sigma^+$(polarized) direction revealed negative parity, and thus established $J^P = 1/2^-$.

A REVIEW GOES HERE – Check our WWW List of Reviews

### $\Lambda(1405)$ REGION POLE POSITIONS

**REAL PART**

| VALUE (MeV) | DOCUMENT ID | | TECN |
|---|---|---|---|
| • • • We do not use the following data for averages, fits, limits, etc. • • • | | | |
| $1429^{+8}_{-7}$ | [1] MAI | 15 | DPWA |
| $1325^{+15}_{-15}$ | [2] MAI | 15 | DPWA |
| $1434^{+2}_{-2}$ | [3] MAI | 15 | DPWA |
| $1330^{+4}$ | [4] MAI | 15 | DPWA |

Citation: C. Patrignani et al. (Particle Data Group), Chin. Phys. C, 40, 100001 (2016)

## $\Sigma(1385)\ 3/2^+$

$I(J^P) = 1(\frac{3}{2}^+)$ Status: ****

Discovered by ALSTON 60. Early measurements of the mass and width for combined charge states have been omitted. They may be found in our 1984 edition Reviews of Modern Physics **56** S1 (1984).

We average only the most significant determinations. We do not average results from inclusive experiments with large backgrounds or results which are not accompanied by some discussion of experimental resolution. Nevertheless systematic differences between experiments remain. (See the ideograms in the Listings below.) These differences could arise from interference effects that change with production mechanism and/or beam momentum. They can also be accounted for in part by differences in the parametrizations employed. (See BORENSTEIN 74 for a discussion on this point.) Thus BORENSTEIN 74 uses a Breit-Wigner with energy-independent width, since a $P$-wave was found to give unsatisfactory fits. CAMERON 78 uses the same form. On the other hand HOLMGREN 77 obtains a good fit to their $\Lambda\pi$ spectrum with a $P$-wave Breit-Wigner, but includes the partial width for the $\Sigma\pi$ decay mode in the parametrization. AGUILAR-BENITEZ 81D gives masses and widths for five different Breit-Wigner shapes. The results vary considerably. Only the best-fit $S$-wave results are given here.

### $\Sigma(1385)$ MASSES

**$\Sigma(1385)^+$ MASS**

| VALUE (MeV) | EVTS | DOCUMENT ID | | TECN | COMMENT |
|---|---|---|---|---|---|
| **1382.80±0.35 OUR AVERAGE** Error includes scale factor of 1.9. See the ideogram below. | | | | | |
| $1383.2 \pm 0.9\ ^{+0.1}_{-1.5}$ | | AGAKISHIEV | 12 | SPEC | $pp \to \Sigma(1385)^+ K^+ n$, 3.5 GeV |
| $1384.1 \pm 0.7$ | 1897 | BAUBILLIER | 84 | HBC | $K^- p$ 8.25 GeV/$c$ |
| $1384.5 \pm 0.5$ | 5256 | AGUILAR-... | 81D | HBC | $K^- p \to \Lambda\pi\pi$ 4.2 GeV/$c$ |
| $1383.0 \pm 0.4$ | 9361 | AGUILAR-... | 81D | HBC | $K^- p \to \Lambda 3\pi$ 4.2 GeV/$c$ |
| $1381.9 \pm 0.3$ | 6900 | CAMERON | 78 | HBC | $K^- p$ 0.96–1.36 GeV/$c$ |
| $1381 \pm 1$ | 6846 | BORENSTEIN | 74 | HBC | $K^- p$ 2.18 GeV/$c$ |

# Applications

- $\Lambda(1405)$ is dominated by KN interaction

- A similar mechanism can be responsible for the generation of $K^-pp$ bound states. See for example, S. Ajimura et al arXiv:1805.12275 [nucl-ex].

- The equation of state of neutron stars is sensitive to the antikaon condensate and thus to the propagation of antikaons in nuclear medium.

# Method

# Model

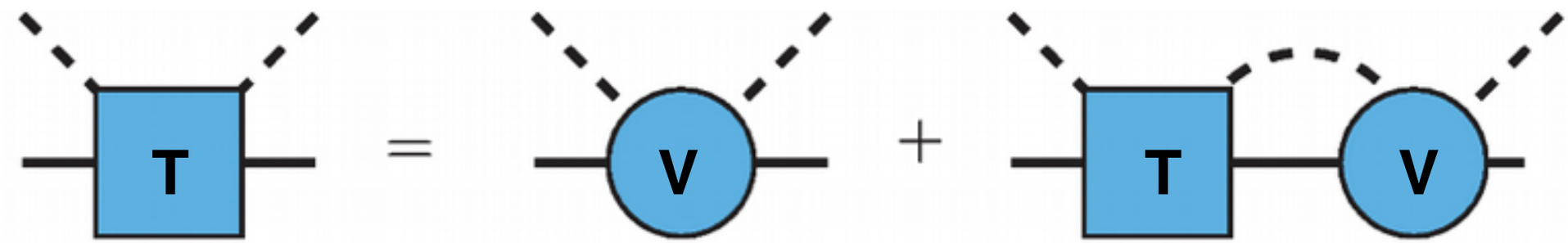


A depiction of the operator form of the Bethe Saltpeter Equation.

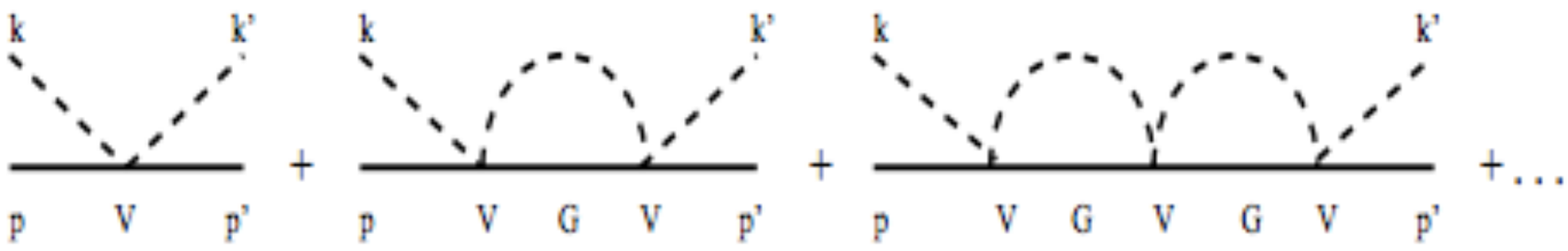


The bubble chain summation caused by iteration of the Bethe Salpeter Ansatz

$$V(\not{q}_2, \not{q}_1; p) = A_{WT}(\not{q}_1 + \not{q}_2) + Born(s) + Born(u)$$
$$+ A_{14}(q_1 \cdot q_2) + A_{57}[\not{q}_1, \not{q}_2] + A_M + A_{811}\Big(\not{q}_2(q_1 \cdot p) + \not{q}_1(q_2 \cdot p)\Big)$$

The chiral expansion of the driving term, V.

# Possible Meson Baryon Interactions for S=-1

| | | | | | | | | | |
|---|---|---|---|---|---|---|---|---|---|
| $\mathbf{K^-p \to K^-p}$ | $\mathbf{K^-p \to \bar{K}^0n}$ | $\mathbf{K^-p \to \pi^0\Lambda}$ | $\mathbf{K^-p \to \pi^0\Sigma^0}$ | $\mathbf{K^-p \to \pi^+\Sigma^-}$ | $\mathbf{K^-p \to \pi^-\Sigma^+}$ | $K^-p \to \eta\Lambda$ | $K^-p \to \eta\Sigma^0$ | $K^-p \to K^+\Xi^-$ | $K^-p \to K^0\Xi^0$ |
| $K^0n \to K^-p$ | $K^0n \to \bar{K}^0n$ | $K^0n \to \pi^0\Lambda$ | $K^0n \to \pi^0\Sigma^0$ | $K^0n \to \pi^+\Sigma^-$ | $K^0n \to \pi^-\Sigma^+$ | $K^0n \to \eta\Lambda$ | $K^0n \to \eta\Sigma^0$ | $K^0n \to K^+\Xi^-$ | $K^0n \to K^0\Xi^0$ |
| $\pi^0\Lambda \to K^-p$ | $\pi^0\Lambda \to \bar{K}^0n$ | $\pi^0\Lambda \to \pi^0\Lambda$ | $\pi^0\Lambda \to \pi^0\Sigma^0$ | $\pi^0\Lambda \to \pi^+\Sigma^-$ | $\pi^0\Lambda \to \pi^-\Sigma^+$ | $\pi^0\Lambda \to \eta\Lambda$ | $\pi^0\Lambda \to \eta\Sigma^0$ | $\pi^0\Lambda \to K^+\Xi^-$ | $\pi^0\Lambda \to K^0\Xi^0$ |
| $\pi^0\Sigma^0 \to K^-p$ | $\pi^0\Sigma^0 \to \bar{K}^0n$ | $\pi^0\Sigma^0 \to \pi^0\Lambda$ | $\pi^0\Sigma^0 \to \pi^0\Sigma^0$ | $\pi^0\Sigma^0 \to \pi^+\Sigma^-$ | $\pi^0\Sigma^0 \to \pi^-\Sigma^+$ | $\pi^0\Sigma^0 \to \eta\Lambda$ | $\pi^0\Sigma^0 \to \eta\Sigma^0$ | $\pi^0\Sigma^0 \to K^+\Xi^-$ | $\pi^0\Sigma^0 \to K^0\Xi^0$ |
| $\pi^+\Sigma^- \to K^-p$ | $\pi^+\Sigma^- \to \bar{K}^0n$ | $\pi^+\Sigma^- \to \pi^0\Lambda$ | $\pi^+\Sigma^- \to \pi^0\Sigma^0$ | $\pi^+\Sigma^- \to \pi^+\Sigma^-$ | $\pi^+\Sigma^- \to \pi^-\Sigma^+$ | $\pi^+\Sigma^- \to \eta\Lambda$ | $\pi^+\Sigma^- \to \eta\Sigma^0$ | $\pi^+\Sigma^- \to K^+\Xi^-$ | $\pi^+\Sigma^- \to K^0\Xi^0$ |
| $\pi^-\Sigma^+ \to K^-p$ | $\pi^-\Sigma^+ \to \bar{K}^0n$ | $\pi^-\Sigma^+ \to \pi^0\Lambda$ | $\pi^-\Sigma^+ \to \pi^0\Sigma^0$ | $\pi^-\Sigma^+ \to \pi^+\Sigma^-$ | $\pi^-\Sigma^+ \to \pi^-\Sigma^+$ | $\pi^-\Sigma^+ \to \eta\Lambda$ | $\pi^-\Sigma^+ \to \eta\Sigma^0$ | $\pi^-\Sigma^+ \to K^+\Xi^-$ | $\pi^-\Sigma^+ \to K^0\Xi^0$ |
| $\eta\Lambda \to K^-p$ | $\eta\Lambda \to \bar{K}^0n$ | $\eta\Lambda \to \pi^0\Lambda$ | $\eta\Lambda \to \pi^0\Sigma^0$ | $\eta\Lambda \to \pi^+\Sigma^-$ | $\eta\Lambda \to \pi^-\Sigma^+$ | $\eta\Lambda \to \eta\Lambda$ | $\eta\Lambda \to \eta\Sigma^0$ | $\eta\Lambda \to K^+\Xi^-$ | $\eta\Lambda \to K^0\Xi^0$ |
| $\eta\Sigma^0 \to K^-p$ | $\eta\Sigma^0 \to \bar{K}^0n$ | $\eta\Sigma^0 \to \pi^0\Lambda$ | $\eta\Sigma^0 \to \pi^0\Sigma^0$ | $\eta\Sigma^0 \to \pi^+\Sigma^-$ | $\eta\Sigma^0 \to \pi^-\Sigma^+$ | $\eta\Sigma^0 \to \eta\Lambda$ | $\eta\Sigma^0 \to \eta\Sigma^0$ | $\eta\Sigma^0 \to K^+\Xi^-$ | $\eta\Sigma^0 \to K^0\Xi^0$ |
| $K^+\Xi^- \to K^-p$ | $K^+\Xi^- \to \bar{K}^0n$ | $K^+\Xi^- \to \pi^0\Lambda$ | $K^+\Xi^- \to \pi^0\Sigma^0$ | $K^+\Xi^- \to \pi^+\Sigma^-$ | $K^+\Xi^- \to \pi^-\Sigma^+$ | $K^+\Xi^- \to \eta\Lambda$ | $K^+\Xi^- \to \eta\Sigma^0$ | $K^+\Xi^- \to K^+\Xi^-$ | $K^+\Xi^- \to K^0\Xi^0$ |
| $K^0\Xi^0 \to K^-p$ | $K^0\Xi^0 \to \bar{K}^0n$ | $K^0\Xi^0 \to \pi^0\Lambda$ | $K^0\Xi^0 \to \pi^0\Sigma^0$ | $K^0\Xi^0 \to \pi^+\Sigma^-$ | $K^0\Xi^0 \to \pi^-\Sigma^+$ | $K^0\Xi^0 \to \eta\Lambda$ | $K^0\Xi^0 \to \eta\Sigma^0$ | $K^0\Xi^0 \to K^+\Xi^-$ | $K^0\Xi^0 \to K^0\Xi^0$ |

Possible channels for S=-1 interactions. The data that exists in the energy region of interest is shown in red.

# Fit to the Data: Old Data

| | |
|---|---|
| $\chi^2_{\rm dof}$ | 1.10 (62/30/8%) |
| $\lvert\Sigma\rvert$ [GeV$^{-14}$] | 0.106 |

| $a_{1-6}$ | $b_{1-11}$ [GeV$^{-1}$] |
|---|---|
| $+0.44^{+0.28}_{-0.14}$ | $-0.34^{+0.11}_{-0.04}$ |
| $+2.04^{+1.37}_{-0.50}$ | $+0.29^{+0.21}_{-0.18}$ |
| $+0.14^{+0.15}_{-0.20}$ | $-0.62^{+0.04}_{-0.06}$ |
| $-0.95^{+0.30}_{-0.31}$ | $-0.02^{+0.16}_{-0.14}$ |
| $-0.75^{+0.16}_{-0.45}$ | $+0.24^{+0.06}_{-0.11}$ |
| $-1.99^{+0.30}_{-3.59}$ | $-0.82^{+0.31}_{-0.09}$ |
| | $-1.32^{+0.44}_{-0.04}$ |
| $b_{0,D,F}$ [GeV$^{-1}$] | $-0.01^{+0.02}_{-0.10}$ |
| $-0.50^{+0.01}_{-0.01}$ | $+0.04^{+0.22}_{-0.14}$ |
| $+0.08^{+0.01}_{-0.01}$ | $+0.15^{+0.05}_{-0.06}$ |
| $-0.22^{+0.01}_{-0.01}$ | $+0.40^{+0.13}_{-0.05}$ |

In addition, we fit to threshold data including data from the SIDDHARTA Experiment

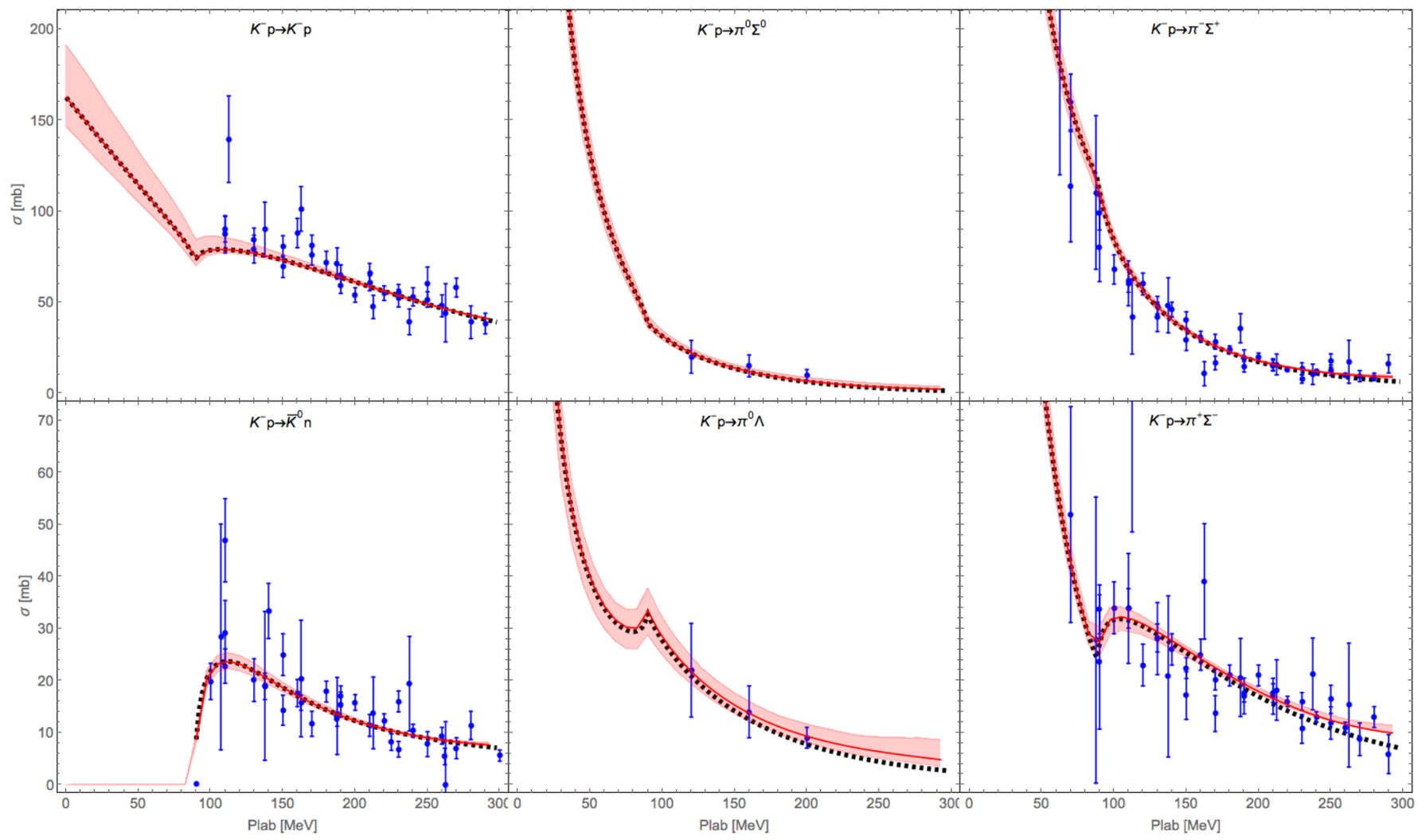


Total cross sections fitted by the model. The dashed black line shows the contribution of the s-wave part of the amplitude only.

# Fit to the Data: New Data

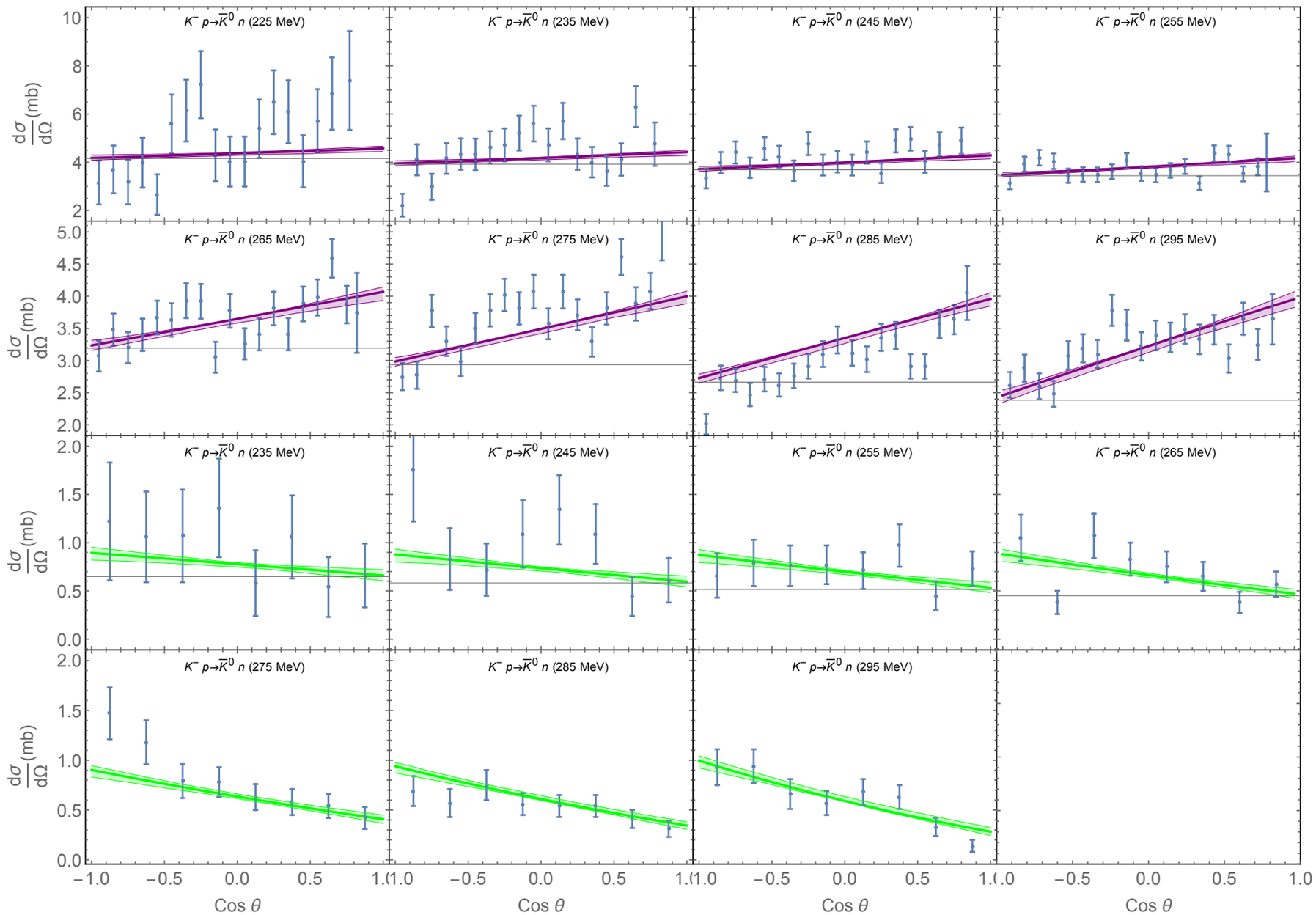


Differential cross sections fitted by the model.

# More Data

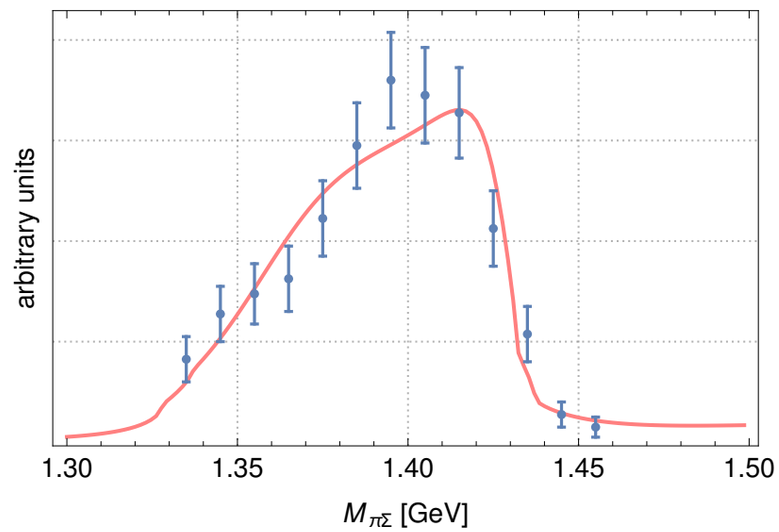


Fit of the generic couplings K−p→Σ(1660)π−and Σ(1660)→(π−Σ+)π+to the invariant mass distribution in arbitrary units.
R. J. Hemingway, Nucl. Phys. B253, 742 (1985).

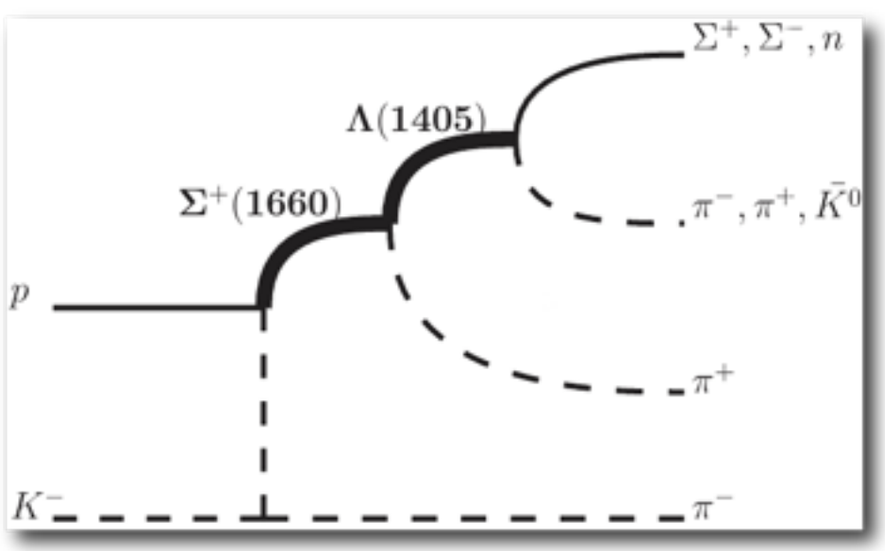


Fit ($\chi^2_{pp}$= 1.07) to theπ Σ invariant mass distribution ($M_{inv}$) from γp→K+(πΣ) reaction.
K. Moriya et al. (CLAS), Phys. Rev. C87, 035206 (2013), arXiv:1301.5000 [nucl-ex].

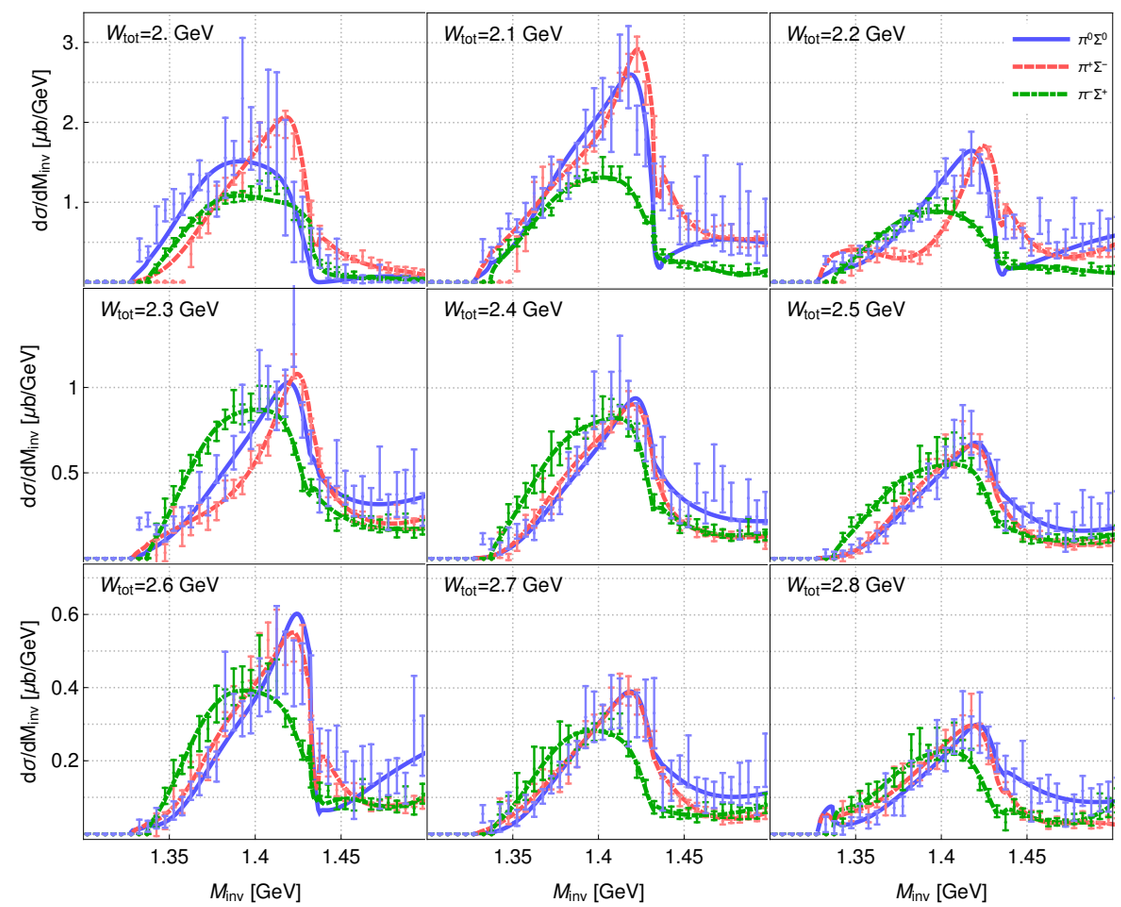

# Predictions

# PWA Amplitudes

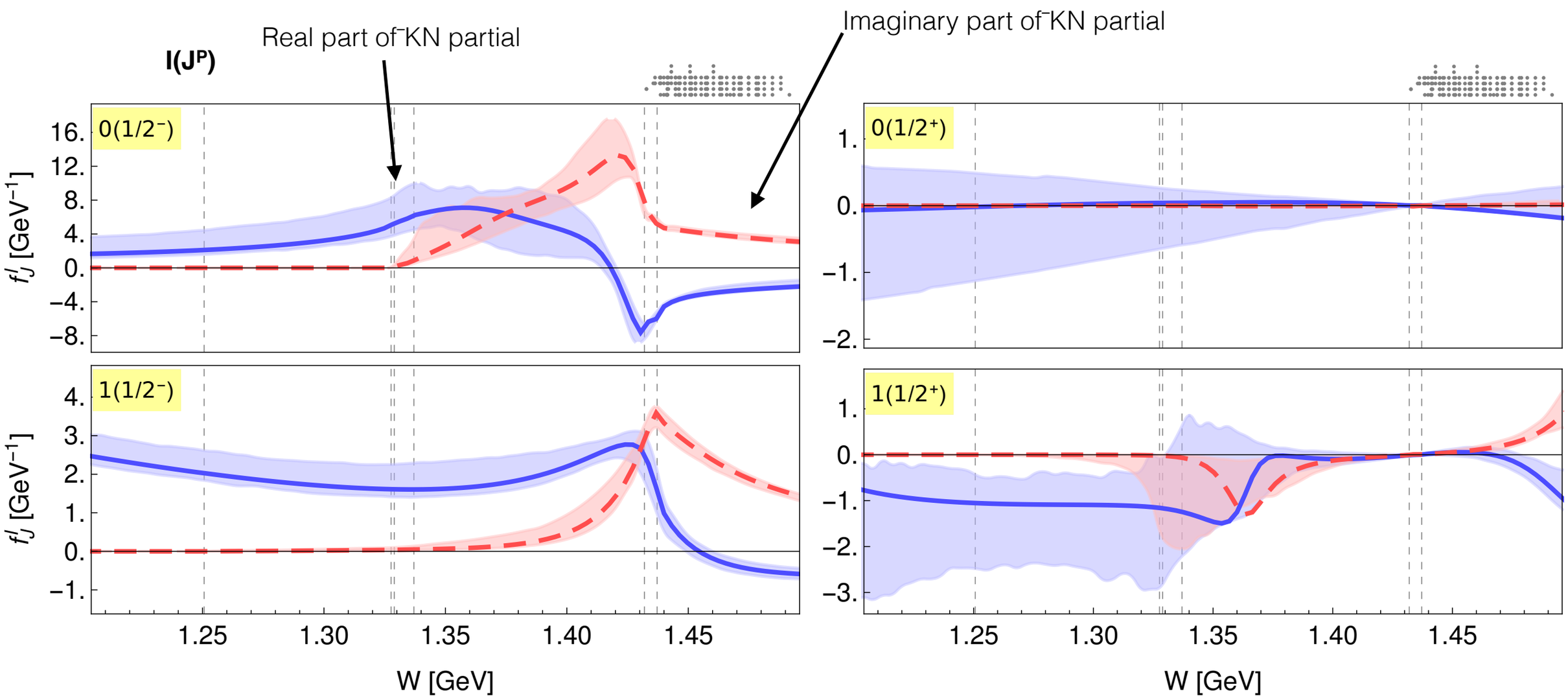

# Λ(1405)

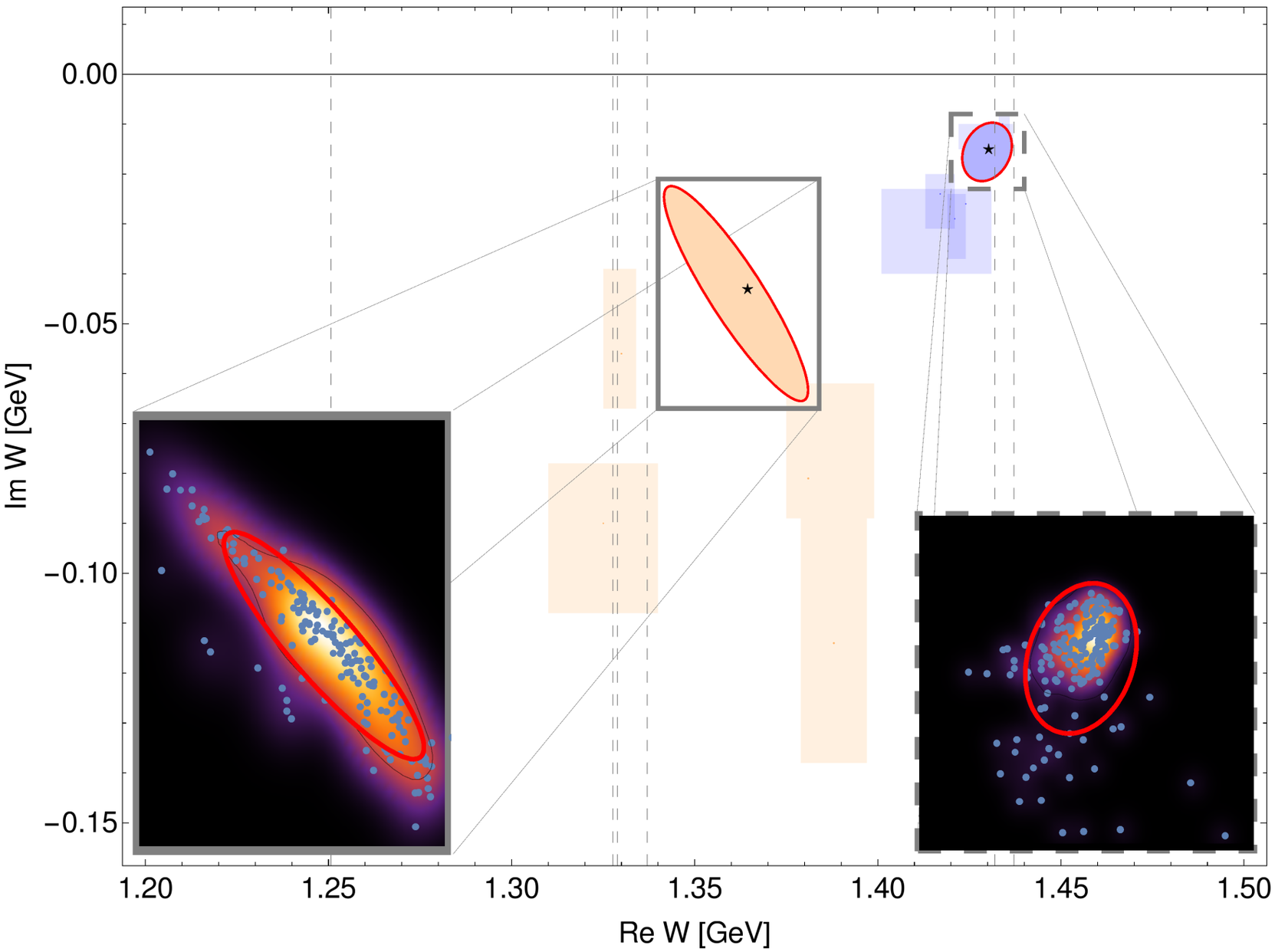


Left: Pole positions (black stars) for the 0(1/2−). The error ellipses are from a re-sampling procedure shown explicitly in the corresponding insets. The shaded squares show the prediction from other literature for the narrow (blue) and broad (orange) pole of Λ(1405)

Below: A plot of the amplitude in the complex plane that shows the two peaks.

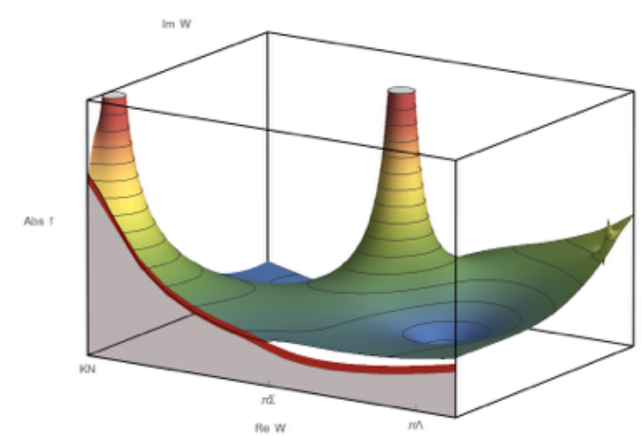

# An Anomalous Structure

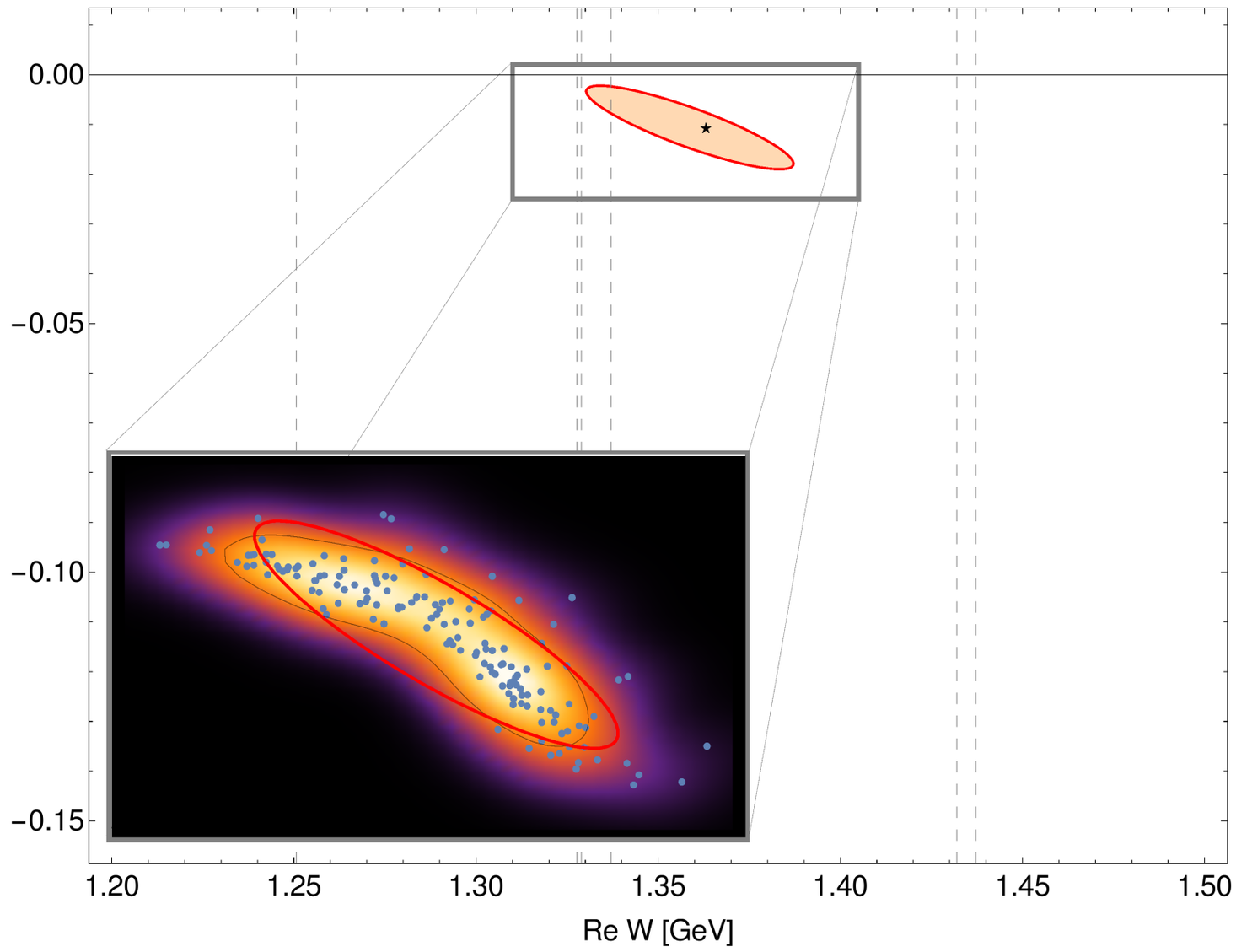


Left: A representation of the position of a pole in the best fit of our model in the 1(1/2⁺) Channel.

Below: The amplitudes of the couplings for the poles observed in the best fit.

| $I(J^P)$ | | $0(1/2^-)$ | $0(1/2^-)$ | $1(1/2^+)$ |
|---|---|---|---|---|
| Pole position [MeV] | | $1430 - 15i$ | $1360 - 43i$ | $1360 - 11i$ |
| Covariance [MeV$^2$] | | $\begin{pmatrix} +20.0 & +3.7 \\ & +14.9 \end{pmatrix}$ | $\begin{pmatrix} +169 & -166 \\ & +202 \end{pmatrix}$ | $\begin{pmatrix} +354 & -91 \\ & +31 \end{pmatrix}$ |
| Couplings [GeV] | $g_{K^-p}$ | $0.34^{+0.10}_{-0.05}$ | $0.35^{+0.06}_{-0.03}$ | $0.10^{+0.05}_{-0.03}$ |
| | $g_{\bar{K}^0 n}$ | $0.32^{+0.10}_{-0.05}$ | $0.35^{+0.06}_{-0.04}$ | $0.10^{+0.04}_{-0.03}$ |
| | $g_{\pi^0\Lambda}$ | – | – | $0.19^{+0.03}_{-0.03}$ |
| | $g_{\pi^0\Sigma^0}$ | $0.19^{+0.03}_{-0.02}$ | $0.39^{+0.04}_{-0.03}$ | – |
| | $g_{\pi^+\Sigma^-}$ | $0.19^{+0.03}_{-0.02}$ | $0.40^{+0.04}_{-0.03}$ | $0.11^{+0.06}_{-0.07}$ |
| | $g_{\pi^-\Sigma^+}$ | $0.19^{+0.03}_{-0.02}$ | $0.38^{+0.04}_{-0.03}$ | $0.09^{+0.06}_{-0.06}$ |
| | $g_{\eta\Lambda}$ | $0.22^{+0.23}_{-0.09}$ | $0.30^{+0.10}_{-0.07}$ | – |
| | $g_{\eta\Sigma^0}$ | – | – | $0.13^{+0.25}_{-0.07}$ |
| | $g_{K^+\Xi^-}$ | $0.05^{+0.03}_{-0.03}$ | $0.02^{+0.02}_{-0.01}$ | $0.08^{+0.07}_{-0.06}$ |
| | $g_{K^0\Xi^0}$ | $0.06^{+0.03}_{-0.03}$ | $0.02^{+0.02}_{-0.01}$ | $0.08^{+0.07}_{-0.06}$ |

# Analysis

# Possible Explanations of the Anomalous Structure

When a structure is observed in a good fit to good data and does not have the quantum numbers of any known state, categorically speaking there are three possibilities.

1. It's present because the data demonstrate that there exists an undiscovered state in nature.

2. It's present because the data require the model to account for something it isn't currently accounting for.

3. It's completely arbitrary; it's existence does not improve the fit in any way.

# Lasso Test of Robustness

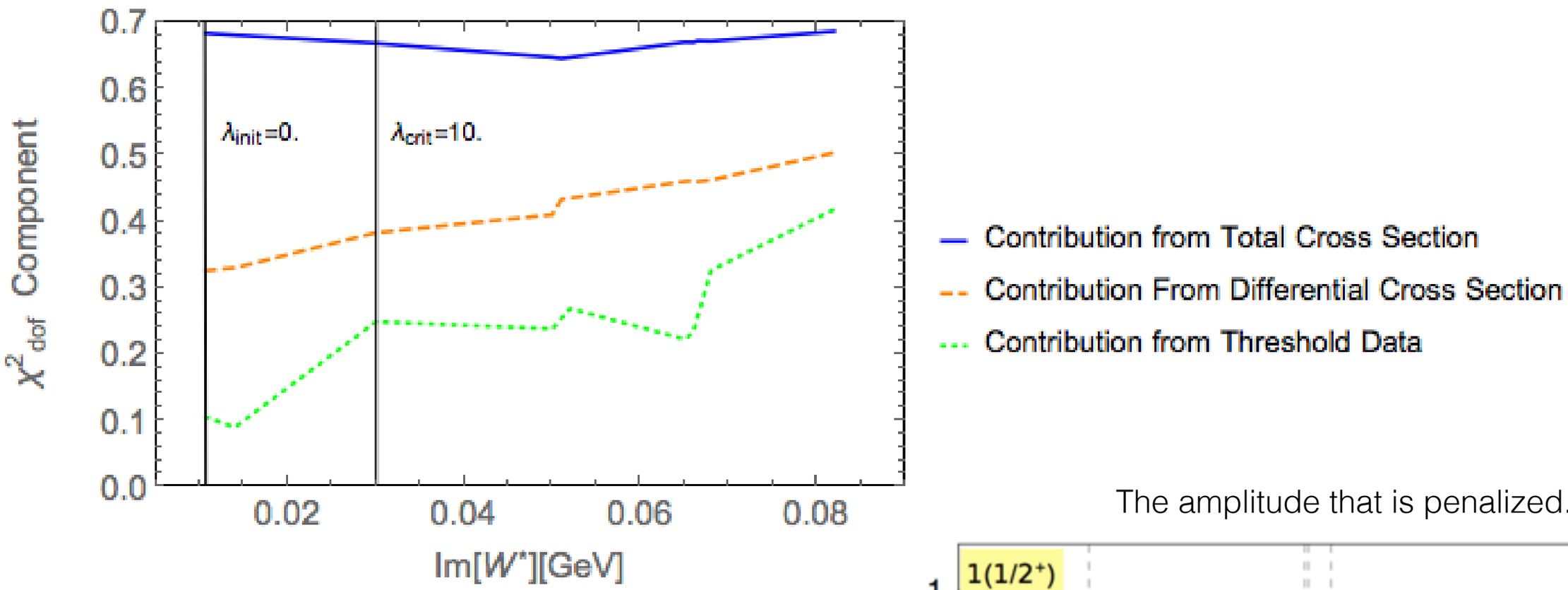


Plot of Lasso (Least Absolute Shrinkage and Selection Operator) Method.

The amplitude that is penalized.

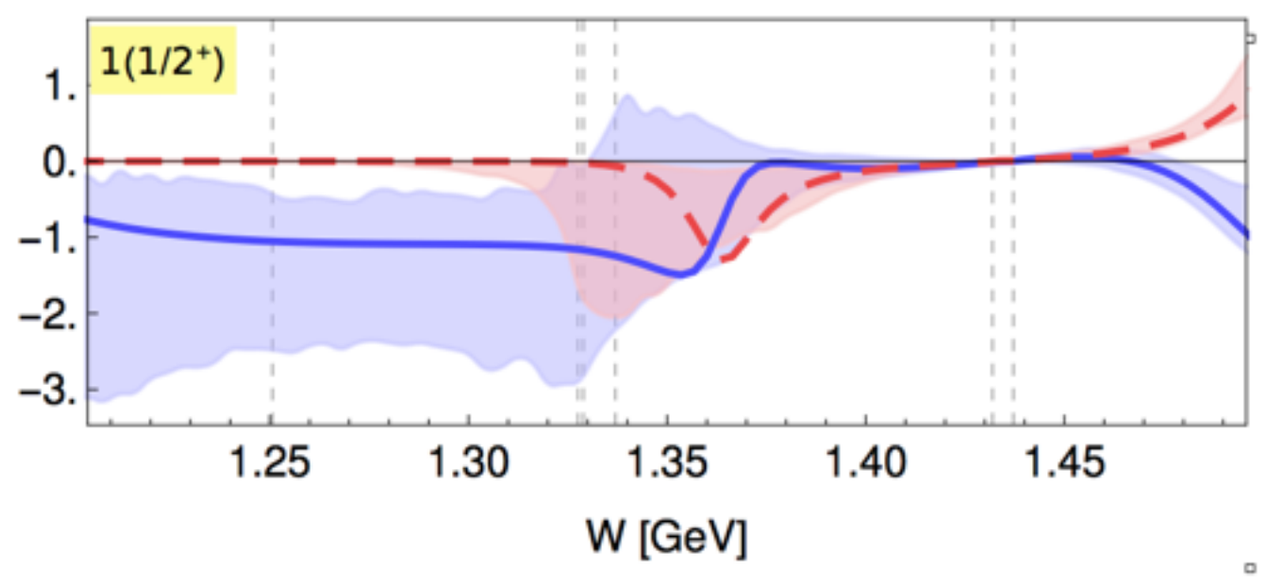

# Possible Explanations of the Anomalous Structure

When a structure is observed in a good fit to the data and does not have the quantum numbers of any known state, categorically speaking there are three possibilities.

1. It's present because the data demonstrate that there exists an undiscovered state in nature.

2. It's present because the data require the model to account for something it isn't currently accounting for.

3. ~~It's completely arbitrary; it's existence does not improve the fit in any way.~~

# Σ(1385)

$$\frac{d\sigma}{d\Omega} = |f_{0+} + z(f_{1-} + 2f_{1+})|^2 + |f_{1-} - f_{1+}|^2(1-z)^2$$

Real Formula for the differential cross section

$$\frac{d\sigma}{d\Omega} = |f_{0+} + z(2f_{1-} + f_{1+})|^2 + |f_{1-} - f_{1+}|^2(1-z)^2$$

Reversed Formula for the differential cross section

The partial waves of the best fit. We additionally include a black line to show the best fit when the partial waves are reversed.

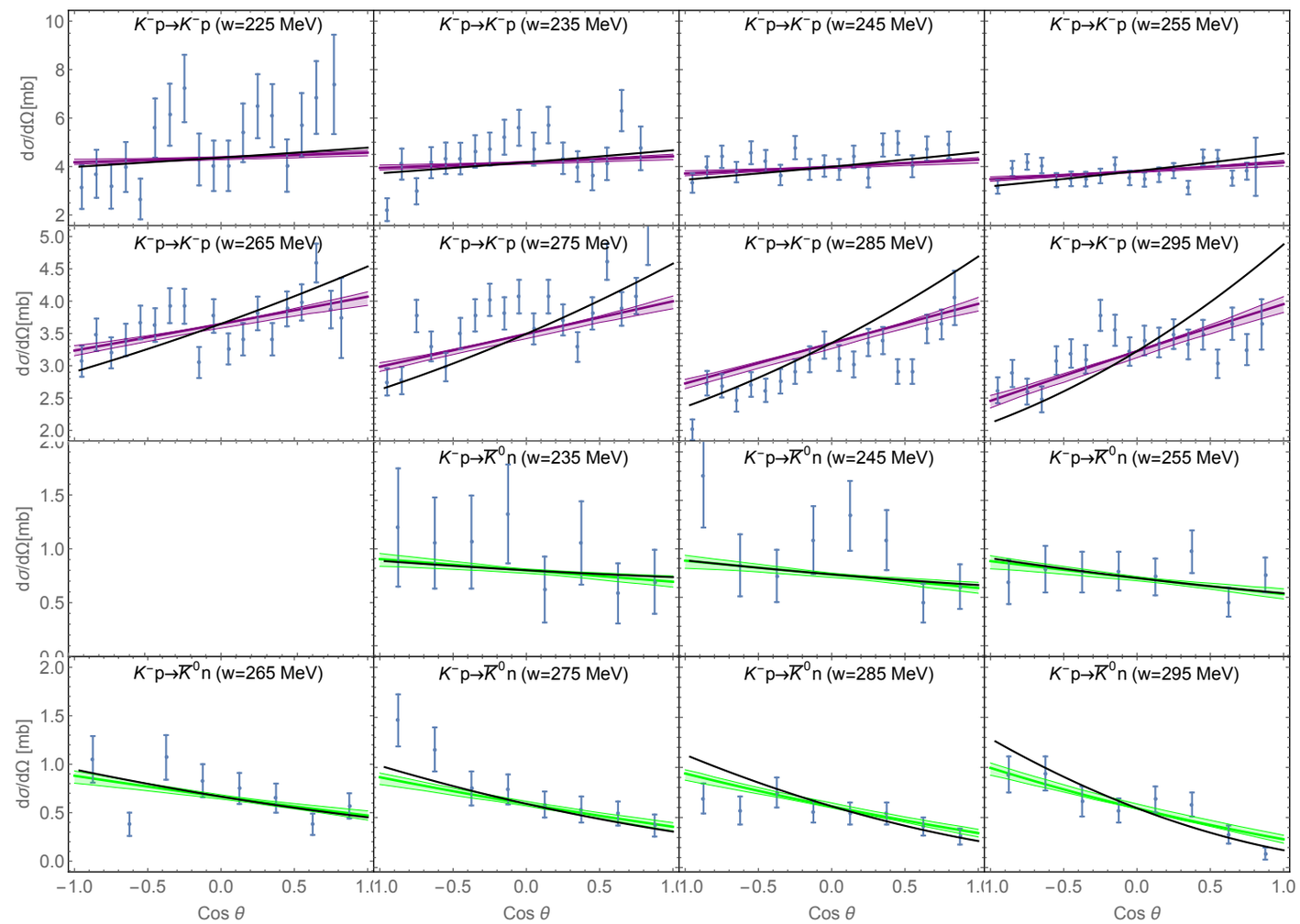


$$16\pi W f_{\ell\pm}(W) = (E+m)\{A_\ell + (W-m)B_\ell\} + (E-m)\{-A_{\ell\pm1} + (W+m)B_{\ell\pm1}\}$$

# Possible Explanations of the Anomalous Structure

When a structure is observed in a good fit to the data and does not have the quantum numbers of any known state, categorically speaking there are three possibilities.

1. ~~It's present because the data demonstrate that there exists an undiscovered state in nature.~~

2. It's present because the data require the model to account for something it isn't currently accounting for.

3. ~~It's completely arbitrary; it's existence does not improve the fit in any way.~~

# Summary

- The Mai-Meissner Model is fit to differential cross section as well as older data. This constitutes the first ever simultaneous fit of all data without explicit resonances.

- Both poles of the Λ(1405) were reproduced

- A new anomalous structure was observed that didn't have the right parity for the Σ(1385).

- This statistically robust state likely exists because the differential cross section data demand a p-wave resonance and a NLO model cannot give it the right J.

Thank You